Nonlinear Dyn (2010) 59: 329–338
DOI 10.1007/s11071-009-9542-8

ORIGINAL PAPER

Hopf bifurcation and chaotic motions of a tubular cantilever subject to cross flow and loose support

L. Wang · Q. Ni

Received: 12 February 2009 / Accepted: 28 May 2009 / Published online: 6 June 2009

Abstract The Hopf bifurcation and chaotic motions of a tubular cantilever impacting on loose support is studied using an analytic model that involves delay differential equations. By using the damping-controlled mechanism, a single flexible cantilever in an otherwise rigid square array of cylinders is analyzed. The analytical model, after Galerkin discretization to five d.o.f., exhibits interesting dynamical behavior. Numerical solutions show that, with increasing flow beyond the critical, the amplitude of motion grows until impacting with the loose support placed at the tip end of the cylinder occurs; more complex motions then arise, leading to chaos and quasi-periodic motions for a sufficiently high flow velocity. The effect of location of the loose support on the global dynamics of the system is also investigated.

Keywords Hopf bifurcation · Chaotic motion · Cantilever · Cross flow · Loose support

1 Introduction

The instabilities and vibrations of loosely supported cylinders (or tubes) subjected to cross flow have been one interesting subject of investigations by researchers in the power generating industry (including, e.g., steam generators, boilers, condensers, etc.) for several decades. Arrays (or bundles) of cylinders subject to cross flow are known to be possibly subject to fluid elastic instabilities at sufficiently high flow velocities. Some of these instabilities have been linked to a negative damping mechanism arising from the fluid dynamic forces acting on the cylinders. Since this damping may be negative, work is done by the fluid on the cylinders. The fluid elastic instabilities can cause severe damage to the tubular cylinders: the resultant high-amplitude and high-frequency vibration may sometimes cause cylinder impact onto loose supports and always wear with loose supports [1], eventually leading to breakdowns.

Tubular cylinders within steam generators are always positively supported (usually clamped) at both ends. In heat exchangers, sometimes the tubular cylinders are threaded through the baffle plates (i.e., loose supports) through holes. The clearances between the cylinder and the loose supports permit easy threading and allow for thermal expansion. The main function of the baffle plates is to direct the flow and to support the cylinders. One type of loose supports is the tube support plate (TSP) which comprises a flat plate with circular holes for the cylinders to pass through; see Fig. 1(a). A second type of loose supports consists of two parallel bars, known as antivibration bars (AVBs); see Fig. 1(b). Therefore, it seems that the AVBs limit

L. Wang (✉) · Q. Ni
Department of Mechanics, Huazhong University of Science and Technology, Wuhan 430074, China
e-mail: wanglinfliping@sohu.com

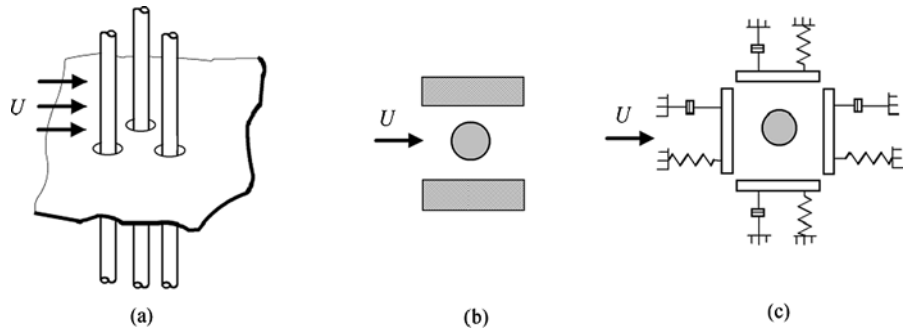

Fig. 1 Three types of loose supports

cylinder motion to one direction; however, as there are clearances between the cylinder and the two parallel bars, the cylinder may also vibrate in the cross-stream direction. A third type of loose supports consists of a number of massless bars arranged around the tube; typically, a square flat-bar (SFB) support is shown in Fig. 1(c).

After some use, crud may be deposited in the clearance, rendering some, but not all, loose-fitting holes into positive supports; also, the fact that the cylinders are not perfectly straight originally and the clamped supports may sometimes be destroyed by flow-induced force or thermal expansion help explain how in a real heat exchanger some clamped supports would be rendered into loose supports after some use.

There are several analytic or semiempirical models for predicting oscillatory fluid-elastic instability (see, e.g., [2–6]). These models are mostly linearized, both in terms of the fluid-dynamic forces acting on the cylinders and in terms of structural motions. The interested reader is referred to Paidoussis' [7] and Chen's [8] discussions of reasonable classifications of these models, as well as to Price's [9] discussion of the possible mechanisms giving rise to the instability.

The nonlinear vibrations of heat exchanger cylinders in cross flow arise from a fluid-induced dynamic instability [10, 11]. In the studies of [10, 11], a clamped-clamped cylinder was supported at midspan by AVBs. It should be noted that the analytic model used in these two papers is that of Price and Paidoussis [3]. Paidoussis and Li [11] demonstrated that chaotic oscillations for a single flexible cylinder with two-span are in fact possible for sufficiently high fluid flow velocities. This two-span cylinder is clamped at both ends and is loosely supported at the middle (Fig. 2). The nonlinearities considered in that paper are those associated with impacting on the loose supports. In 1999, a robust feed back controller design

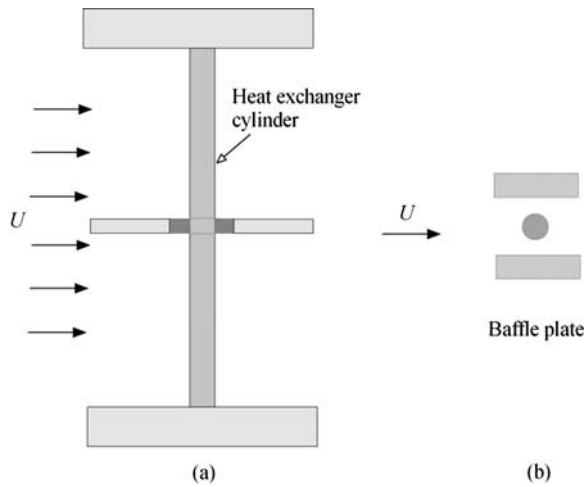

Fig. 2 The analytic model developed in [10–12]: (**a**) top view, (**b**) side view

to suppress flutter-type chaotic vibrations in baffled heat exchanger cylinders was reported by de Bedout et al. [12]. The analytic model developed by Paidoussis and Li [11] was utilized. The feedback controller was realized using a frequency domain loop shaping approach which is well suited for systems with transcendental transfer functions. Cai and Chen [13] analyzed the response of a pinned tube with a loose AVB support. Periodic, quasi-periodic, and chaotic responses were obtained as the flow velocity was varied.

More recently, Hassan and Hayder [14] attempted to formulate a new time-domain model for fluide-lastic instability forces of tubes with loose-supports (SFB) to predict the flow-induced vibrations and associated wear in heat exchangers and steam generators. The mathematical modeling of the tube/support impact used therein was described in detail and verified by Hassan et al. [15]. The loose supports were modeled by a number of massless bars arranged around

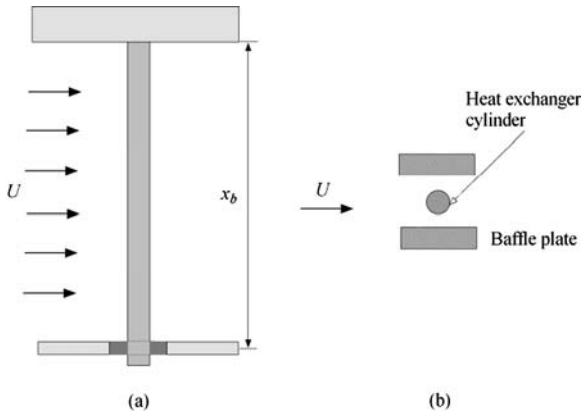

Fig. 3 The analytic model in the current work, showing a single flexible cantilever in an otherwise rigid square array of cylinders: (**a**) top view, (**b**) side view

the tube. Numerical investigations of the response of a single one-span cylinder subjected to cross flow were carried out by FEM. The predicted critical flow velocities were in reasonable agreement with the experimental results.

Under operating conditions, the tubular cylinder is always subjected to high velocity coolant cross-flow. As mentioned in the foregoing, some of the clamped supports may be rendered into loose supports after some use. When the fluid flow velocity is higher than a critical one, the cylinder would impact onto these loose supports, thus introducing strong nonlinearities in the system. Therefore, the present paper is concerned with the dynamics of a one-span cylinder in cross-flow, with the extremes of the cylinder being positively clamped at one end and loosely supported at the other end or close to it; see Fig. 3.

Therefore, it can be seen that the current model is different from that shown in Fig. 2. It will here be assumed for simplicity that motions will be planar and in the direction of the single degree of freedom considered. While the inflow motion of the cylinder does occur in real systems, the tube response is usually dominant in the cross-flow direction. This means that the in-flow-direction motion of the cylinder is not considered in the current work.

The main motivation for this work is to investigate the bifurcations and possible chaotic motions in such a cantilevered system. The dynamics of the system are studied through theoretical analysis and numerical simulation, obtaining bifurcation diagrams and phase portraits and showing some essential results. All the results obtained for a cantilevered system will be compared with that for a supported system analyzed in [11].

2 Analytic model

2.1 The equation of motion

Consider the one-span heat exchanger cylinder in cross-flow in Fig. 3. The single flexible cylinder is surrounded by otherwise rigid cylinders. The system chosen was a square in-line array. One end of the cylinder is rigidly supported and the other one is free. Moreover, there is a loose support close to or at the tip end of the cylinder. The position of the loose support is denoted by x_b. It is assumed that the heat exchanger cylinder moves perpendicular to the flow direction only, as mentioned in the foregoing. The following derivation of the equation of motion for the flexible cylinder subjected to cross flow has been developed in Paidoussis and Li [11] and will be reviewed briefly here.

The equation of motion of the tubular cantilever subject to cross flow may be written in the form

$$EI\frac{\partial^4 w}{\partial x^4} + c\frac{\partial w}{\partial t} + m\frac{\partial^2 w}{\partial t^2} + \delta(x - x_b) f(w) = F(w, \dot{w}, \ddot{w}) \tag{1}$$

where w is the lateral displacement of the cylinder perpendicular to the flow direction, EI is the flexural rigidity of the cylinder, c is the damping coefficient, m is the cylinder mass per unit length, x is the position along the tube, δ is the Dirac delta function, $f(w)$ is the force exerted by the loose support on the cylinder, and $F(w, \dot{w}, \ddot{w})$ is the flow-induced force associated with the cross flow. The flow-induced force F is a function of the cylinder motion and can be generally expressed by [11, 12]

$$F(w, \dot{w}, \ddot{w}) = M\frac{\partial^2 w(x,t)}{\partial t^2} + B\frac{\partial w(x,t)}{\partial t} + Cw(x, t - \Delta t) \tag{2}$$

where

$$M = -\frac{\pi}{4}\rho D^2 C_{\mathrm{ma}}, \quad B = -\frac{1}{2}\rho U D C_{\mathrm{D}},$$
$$C = \frac{1}{2}\rho U^2 D\frac{\partial C_{\mathrm{L}}}{\partial w}, \quad \Delta t = \mu\frac{D}{U},$$

and D is the diameter of the cylinder, ρ and U are defined as the fluid density and velocity, respectively, C_{D} and C_{L} are the drag and lift coefficients, respectively, based on the flow velocity in the gap between the cylinders, C_{ma} is the virtual (or added) mass coefficient of the fluid around the cylinder, and Δt is the time delay between cylinder motions and the fluid dynamic forces generated thereby. For more details on the mechanism of such a time delay, the interested reader is referred to [3].

By introducing the following nondimensional quantities, where L describes the length of the cantilever and λ_1 is the dimensionless eigenvalue of the first mode for a cantilever beam:

$$\eta = \frac{w}{D}, \quad \xi = \frac{x}{L}, \quad \tau = \lambda_1^2 \sqrt{\frac{EI}{mL^4}} t = \Omega_1 t,$$
$$\zeta = \frac{c}{\Omega_1 m},$$

$$\tilde{m} = \frac{m}{\rho D^2}, \quad \tilde{U} = \frac{2\pi U}{D\Omega_1}, \quad \tilde{f} = \frac{f}{m\Omega_1^2},$$
$$\beta = \frac{1}{1 + 4\tilde{m}/\pi C_{\mathrm{ma}}} \tag{3}$$

and then substituting the dimensionless variables (3) and the flow-induced force (2) into (1), the dimensionless equation of motion can be written as

$$\frac{1}{1-\beta}\frac{\partial^2 \eta}{\partial \tau^2}(\xi,\tau) + \left(\zeta + \frac{\tilde{U} C_{\mathrm{D}}}{4\pi\tilde{m}}\right)\frac{\partial \eta}{\partial \tau}(\xi,\tau) + \frac{1}{\lambda_1^4}\frac{\partial^4 \eta}{\partial \xi^4}(\xi,\tau) - \frac{\tilde{U}^2}{8\pi^2\tilde{m}}\frac{\partial C_{\mathrm{L}}}{\partial \eta}\eta(\xi,\tau - T) + \delta(\xi - \xi_b)\tilde{f}(\eta) = 0 \tag{4}$$

It should be noted that T is the dimensionless delay time given by

$$T = \frac{2\pi}{\tilde{U}}$$

for $\mu = 1$.

2.2 Discretization

The infinite dimensional model is discretized by Galerkin's technique, with the cantilever beam eigenfunctions $\phi_i(\xi)$ being used as a suitable set of base functions and $q_i(\tau)$ being the corresponding generalized coordinates; thus,

$$\eta(\xi,\tau) = \sum_{i=1}^{N} \varphi_i(\xi) q_i(\tau) \tag{5}$$

and applying Galerkin's method one obtains

$$\frac{1}{1-\beta}\ddot{q}_i(\tau) + \left(\frac{\delta_i v_i}{\pi} + \frac{\tilde{U} C_{\mathrm{D}}}{4\pi\tilde{m}}\right)\dot{q}_i(\tau) + v_i^2 q_i(\tau) - \frac{\tilde{U}^2}{8\pi^2\tilde{m}}\frac{\partial C_{\mathrm{L}}}{\partial \eta} q_i(\tau - T) + \tilde{f}(\eta_b)\varphi_i(\xi_b) = 0 \tag{6}$$

where $v_i = (\lambda_i/\lambda_1)^2$ are the ratios of the nondimensional natural frequencies to the first one, η_b is the displacement at $\xi = \xi_b$. In the above equation, the viscous damping term has been replaced by the modal damping $\delta_i v_i/\pi$, in which it has been assumed that damping coefficients are small. Thus, the only coupling term in the current modeling is the force $\tilde{f}(\eta_b)$ due to the restraint at the loose supports. If there were no such restraints, then the resulting equations would be decoupled.

For a cantilever system, of course, the derivation of the equation of motion reviewed in the foregoing is quite similar to that for the supported system analyzed by Price and Paidoussis [3]. However, in (6), the values of $\varphi_i(\xi)$ and λ_i (and hence v_i) are quite different between these two models. Therefore, it is expected that the cantilever system may display some essential dynamical behavior different from that of the supported system. The main variable parameters in this work are the dimensionless flow velocity $\tilde{U}$ and the location of the loose support, ξ_b. The fixed values for the other parameters were chosen in accordance to those used in reference [11], calculated by using experiment data:

$$\beta = 0.24, \quad \delta_i = 0.06, \quad C_{\mathrm{D}} = 0.26, \quad \tilde{m} = 3,$$
$$\frac{\partial C_{\mathrm{L}}}{\partial \eta} = -8.1$$

These values correspond to a square heat exchanger tube array (in-line array) with center-to-center pitch-to-diameter ratio $p/D = 1.5$.

Various mathematical models may be used to represent properly the impact forces. The first approximation used by Paidoussis et al. [16] was to model the restraining forces by a cubic spring. Another two representations were that utilized by Paidoussis et al. [17]

involving a smoothened spring model and a trilinear-spring model. In the current work, the restraining force $\tilde{f}(\eta_b)$ is modeled as a cubic spring [12, 16–18],

$$\tilde{f}(\eta_b) = \kappa \eta_b^3 \tag{7}$$

where κ is the stiffness of the cubic spring. In this work, $\kappa = 1000$ in accordance with reference [12].

In what follows, all quantities are understood to be dimensionless, so the tildes on $\tilde{U}$, $\tilde{f}$, and $\tilde{m}$ are henceforth dropped.

3 Bifurcation analysis

In the bifurcation analysis, a similar treatment given in [11] will be utilized. To find the critical flow velocity for the onset of instability, all system parameters are fixed as defined in the foregoing. The main parameter to be gradually increased is the dimensionless flow velocity, U. Eventually, the stable equilibrium (i.e., at the undeformed position) of the cylinder will be lost at a critical value of U. We denote this critical flow velocity as U_{H}. Obviously, for any $U > U_{\mathrm{H}}$, the motion of the cylinder is amplified. However, the nonlinear elements (e.g., the impacting force associated with loose supports) of the system would counterbalance the growth, bringing the cylinder to an oscillatory state with limited amplitudes. A Hopf bifurcation is defined as the loss of the stable equilibrium and onset of amplified oscillation.

According to the bifurcation theory, the critical value, U_{H}, may be calculated by solving the linearized system of (6) by letting $f(\eta_b) = 0$. Upon substituting the physical parameter values given in Sect. 2, one obtains

$$\ddot{q}_i(\tau) + (\alpha_1 + \alpha_2 U)\dot{q}_i(\tau) + \alpha_3 q_i(\tau) + \alpha_4 q_i(\tau - T) = 0 \tag{8}$$

in which $\alpha_1 = 0.0145 v_i$, $\alpha_2 = 0.00524$, $\alpha_3 = 0.76 v_i^2$, $\alpha_4 = 0.026$; and v_i and thus α_i are known for each mode of the cylinder. It can be seen that the above equations are decoupled, and thus can be treated independently. For the ith mode, it is assumed that a solution can be written in the form

$$q_i = q_{i0} e^{\mathrm{j}\omega_i \tau} \tag{9}$$

Table 1 Critical flow velocities U_{H} and non-dimensional natural frequencies ω_i

Mode	U_{H}	ω_i
1	1.785	0.824
2	11.186	5.166
3	31.320	14.465
4	61.374	28.346
5	101.456	46.858

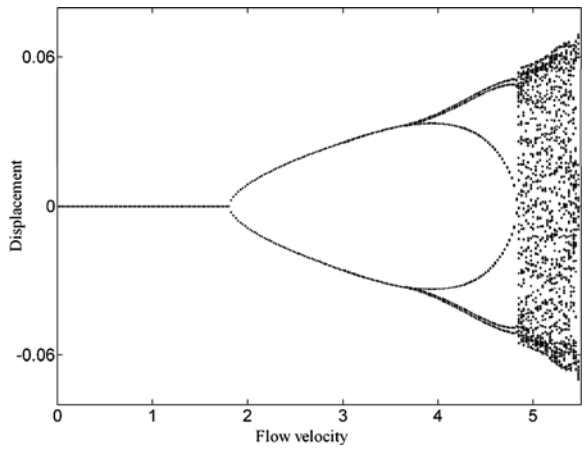

Fig. 4 The bifurcation diagram for the system with loose support at the tip end of the cylinder, showing the tip displacement amplitude in terms of the dimensionless flow velocity, U

where j is the imaginary unit and ω_i is the ith dimensionless eigenfrequency. Substituting (9) into (8) leads to

$$-\omega_i^2 + (\alpha_1 + \alpha_2 U)\mathrm{j}\omega_i + (\alpha_3 + \alpha_4 U^2 e^{-\mathrm{j}\omega_i T}) = 0 \tag{10}$$

At the threshold of the Hopf bifurcation ($U = U_{\mathrm{H}}$), ω_i are required to be purely real, thus

$$\begin{aligned} &-\omega_i^2 + \alpha_3 + \alpha_4 U_{\mathrm{H}}^2 \cos\omega_i T = 0, \\ &(\alpha_1 + \alpha_2 U_{\mathrm{H}})\omega_i - \alpha_4 U_{\mathrm{H}}^2 \sin\omega_i T = 0 \end{aligned} \tag{11}$$

Solutions of the above equations can be easily obtained; the values of U_{H} and ω_i are listed in Table 1.

From Table 1, it can be seen that the critical flow velocity in the first mode is $U_{\mathrm{H1}} = 1.785$. This critical value is the most important, since thereafter an oscillatory state prevails for the cylinder system. Once U

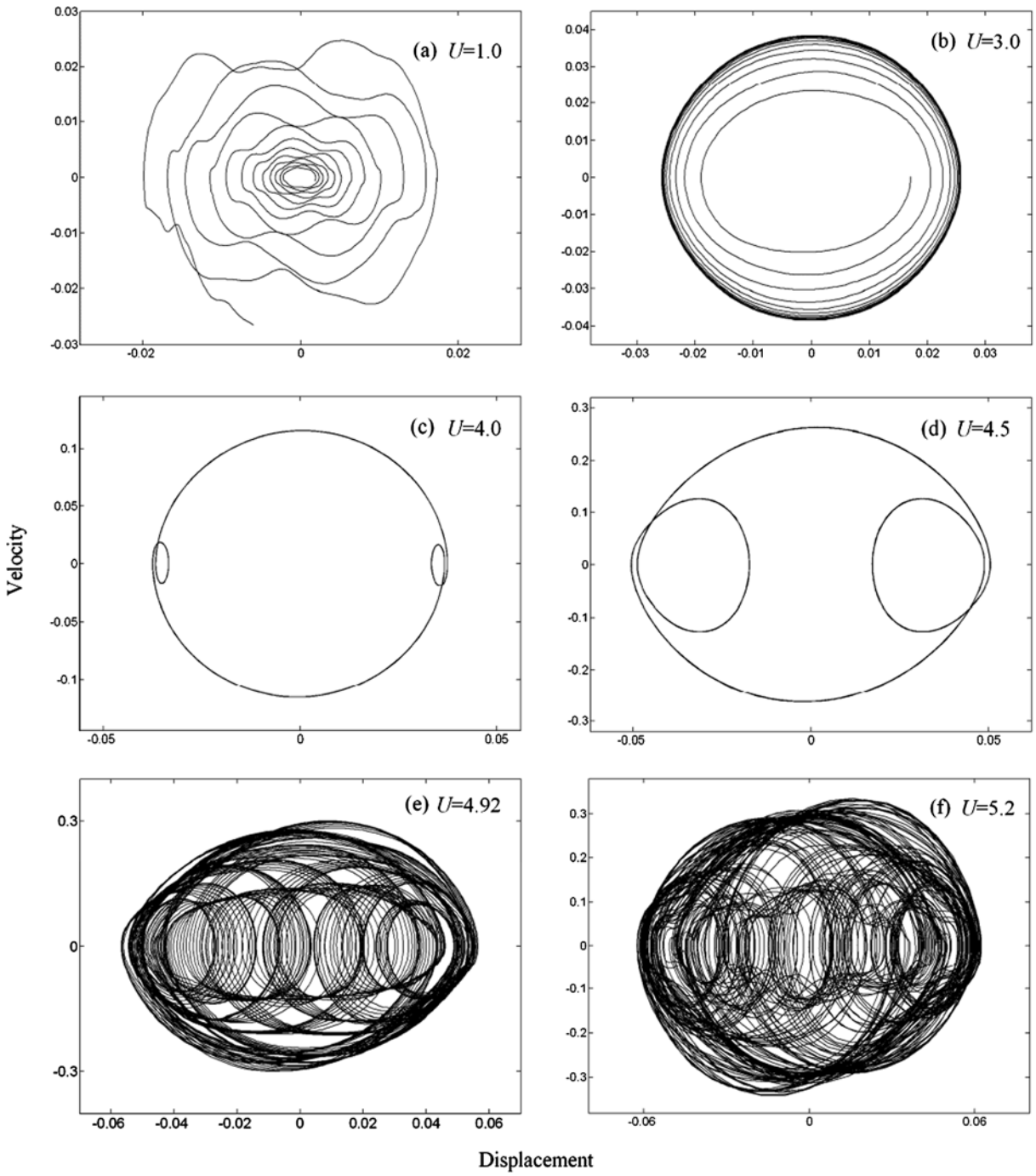

Fig. 5 Phase portraits associated with the bifurcation diagram of Fig. 4, for various values of U

exceeds U_{H}, amplified motions lead to impact with the loose support, whereupon the modes do become coupled. Thus, for $U > U_{\mathrm{H}}$, the higher modes that are still stable provide damping. A balance between the negatively damped unstable modes, dumping energy into the system, and the positively damped stable ones, dissipating it, leads to an oscillation with limited amplitudes.

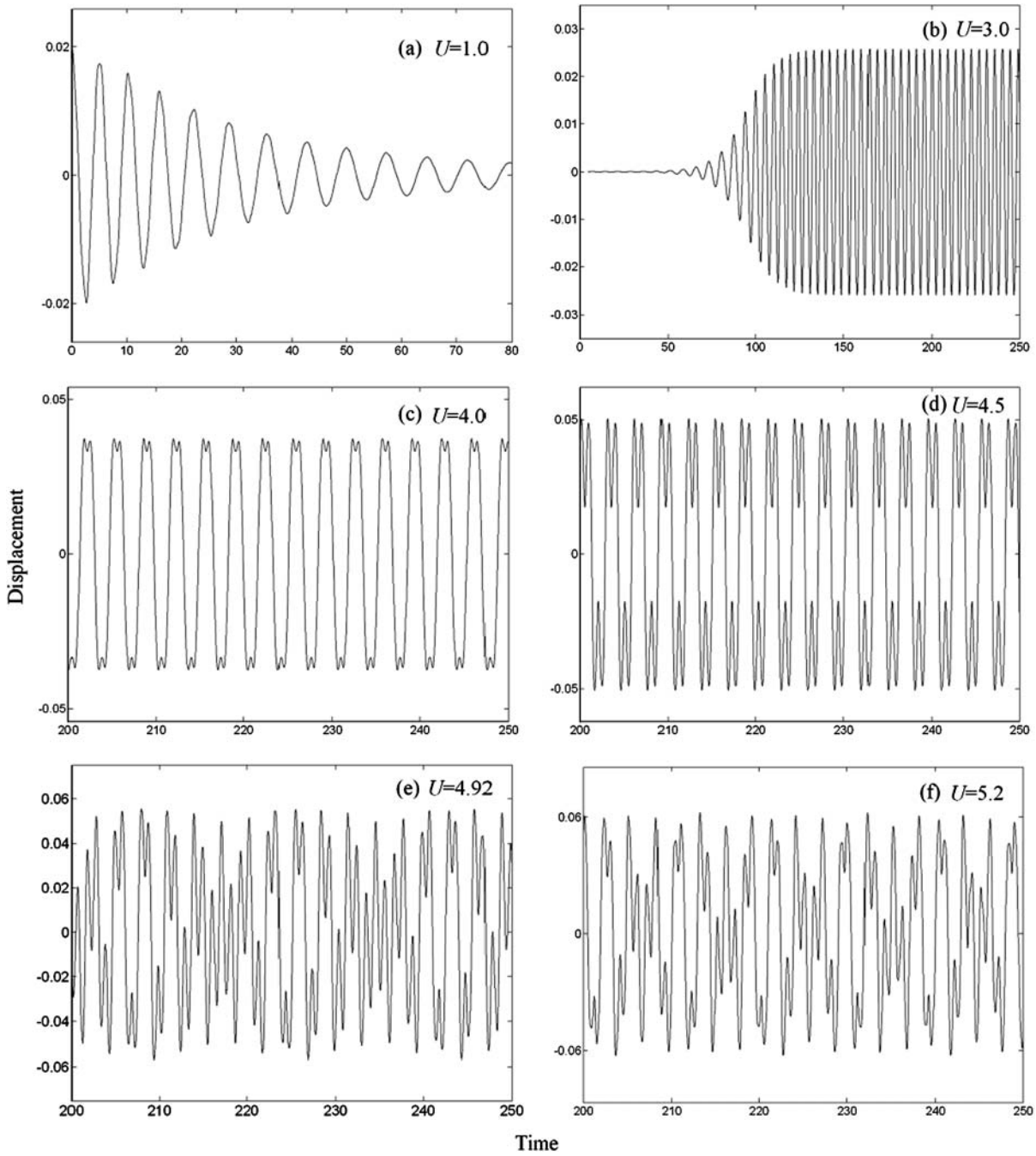

Fig. 6 Time trace diagrams associated with the bifurcation diagram of Fig. 4, for various values of U

Another information shown in Table 1 is that the nondimensional critical flow velocity in the first mode is $U_{\mathrm{H1}} = 1.785$, which is actually the same as that predicted for a clamped-clamped system (see [11]). This, however, dose not mean that the cantilever system and the supported system would lose stability at a same practical (not nondimensional) flow velocity, since λ_1(and hence Ω_1) for the cantilever system is much lower than that for the supported system (see the nondimensional parameters defined in (3)).

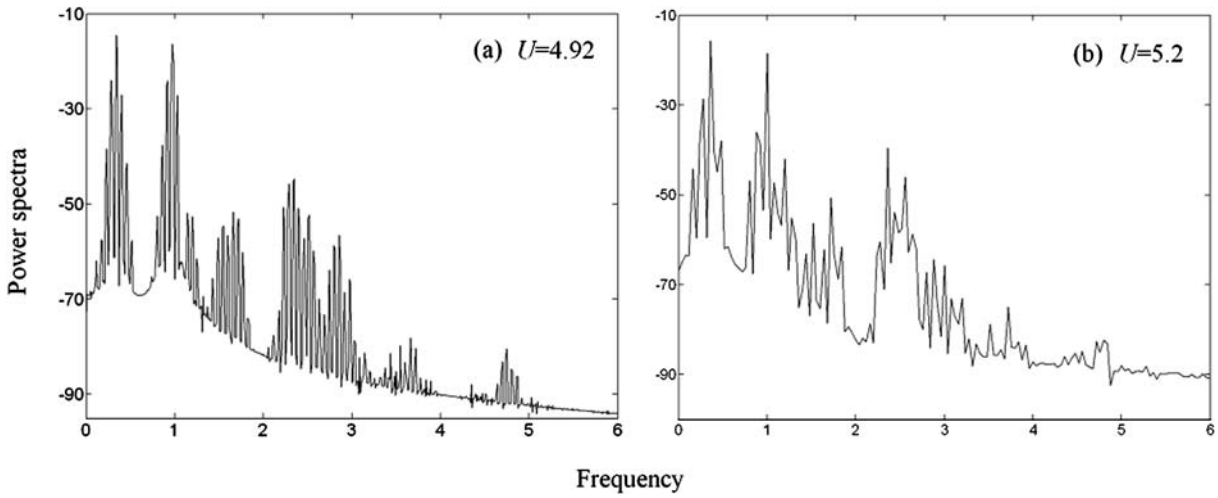

Fig. 7 Power spectrum diagrams associated with the bifurcation diagram of Fig. 4, for two values of U

4 Numerical results

Solutions of (6) were obtained by using a fourth order Runge–Kutta integration algorithm, with a step size of 0.025. As pointed out in [3], simulation results from models with five modes and higher are qualitatively the same both in magnitude and in shape when the integration step size is sufficiently small, and thus five-mode model ($N = 5$) will be used in all the simulations to follow. In the calculations, the initial conditions employed were $q_i = 0.000001, \dot{q}_i = 0$.

The bifurcation diagram for $\xi_b = 1$ is displayed in Fig. 4. In this figure, the displacement plotted in the ordinate is the amplitude of the five-mode approximation of the free-end displacement of the cylinder. It is clearly seen that the Hopf bifurcation occurs at $U_{\mathrm{H}} \approx 1.79$, as predicted earlier by using (11), and thereupon stability is lost, leading to the birth of a limit cycle. Thus, for $U < U_{\mathrm{H}}$, all oscillations will gravitate toward a stable fixed point as time becomes large. It can be also seen that another bifurcation occurs at $U_2 \approx 3.64$, and thereupon a period-3 motion occurs. At $U_3 \approx 4.84$, the period-3 motion disappears and evolves to chaotic motion. Interestingly, there are subregions of quasi-periodic motions embedded within the chaotic region. It is recalled that such subregions of quasi-periodic motions have not been detected in the supported system developed in [11]. In order to have a clear picture of the system dynamics, phase flows were computed for some specially chosen U, and are shown in Fig. 5.

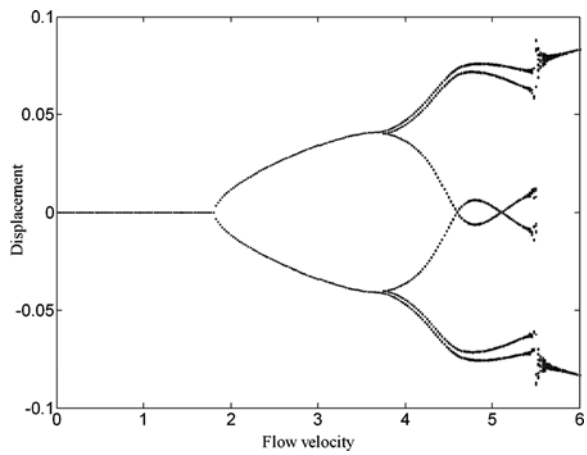

Fig. 8 The bifurcation diagram for the system with loose support at $\xi_b = 0.9$, showing the tip displacement amplitude in terms of the dimensionless flow velocity, U

For $U < U_{\mathrm{H}}$, it is seen in Fig. 5(a) that the origin is a stable fixed point and that the trajectory gravitates towards it. In Fig. 5(b), which is for $U > U_{\mathrm{H}}$, the trajectory is toward the stable limit cycle. Figures 5(c) and (d) show period-3 motions; Figs. 5(e) and (f) show quasi-periodic and chaotic motions, respectively. Sampling results of time traces and power spectrums are shown in Figs. 6 and 7, respectively.

Similar bifurcation diagrams were constructed for $\xi_b = 0.9$ and $\xi_b = 0.8$. First, it is interesting to note that for $\xi_b = 0.9$, a Hopf bifurcation similar to the one shown in Fig. 4 is found, as can be seen in Fig. 8. However, for sufficiently high flow velocities U, no chaotic

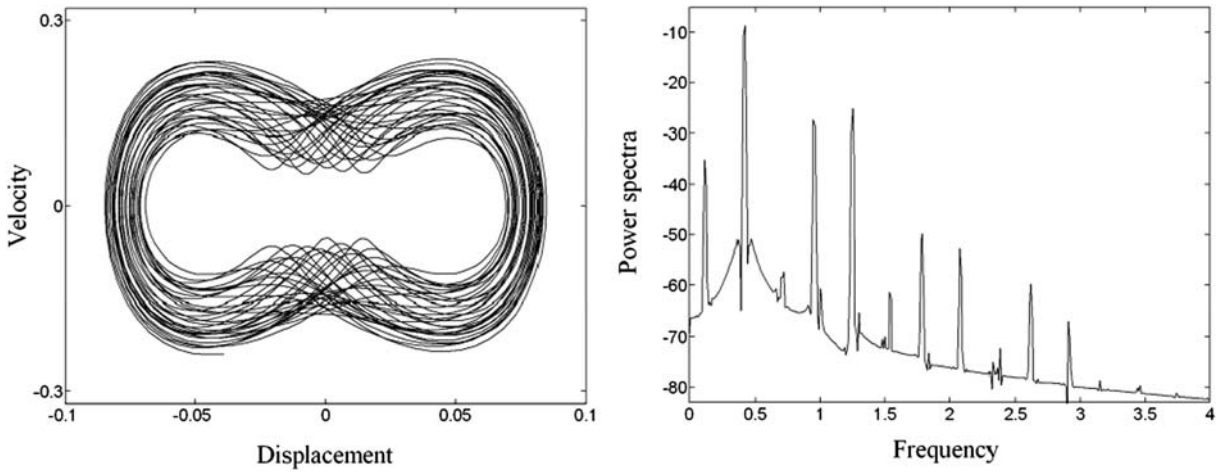

Fig. 9 Phase portrait and power spectrum diagrams associated with the bifurcation diagram of Fig. 8, for $U = 5.55$

motion has been detected. At $U_q \approx 5.52$, a quasi-periodic motion occurs. This type of motion is further demonstrated in the form of power spectrum; see Fig. 9(b). Finally, the quasi-periodic motion evolves to a limit cycle with increasing flow velocities. Second, it is instructive to look at the bifurcation diagram for the case $\xi_b = 0.8$. The result is shown in Fig. 10. In this case, both chaotic and quasi-periodic motions have not been detected, even for sufficiently high flow velocities. Indeed, when $U > U_{\mathrm{H}} \approx 1.79$, a limit cycle motion occurs.

Thus, in the present paper, it has been found that the global dynamics of the cantilever cylinder is sensitive to the location of the loose supports: when the loose support is at the tip end, the cylinder may display quasi-periodic and chaotic motions; when the loose support is far from the tip end, quasi-periodic and chaotic motions may disappear.

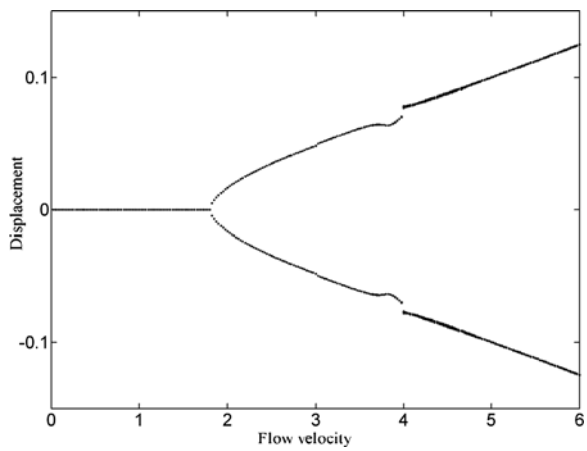

Fig. 10 The bifurcation diagram for the system with loose support at $\xi_b = 0.8$, showing the tip displacement amplitude in terms of the dimensionless flow velocity, U

5 Conclusions

A simple analytic model of a cantilevered cylinder subjected to cross flow and tip loose support, modeled by a cubic spring, has been analyzed and its dynamics studied. By using the damping-controlled mechanism, a single flexible cantilever in an otherwise rigid array of cylinders is considered.

The derivation of the equation of motion has been reviewed briefly first. Based on this equation, the study involves computation of Hopf bifurcation and various post-Hopf nonlinear dynamics of the one-span cylinder. The nondimensional critical flow velocity for the local instability of the flexible cylinder near the static equilibrium position is obtained by assuming a harmonic solution in the discretized linearized model and solving the resulting algebraic equations. It is found that the practical (not nondimensional) critical flow velocity for a cantilever system predicted in the current work is much lower than that for a supported system developed in [11]. Numerical calculations show that, when the loose support is placed at the tip end of the cylinder, with increasing flow beyond the critical, the amplitude of motion grows until impacting with the loose support occurs; more complex motions then

arise, leading to chaotic and quasi-periodic motions for sufficiently high flow velocities. However, when the loose support is placed far from the tip end of the cylinder, quasi-periodic and chaotic motions may disappear.

Thus, compared with the cylinder system with both ends supported, the practical critical flow velocity predicted for the cantilevered system is much lower. This implies that the cantilever system is more unstable in practice. This result is of practical importance also, since the clamped-clamped cylinder may be rendered into a clamped-free system if one of the boundary ends becomes loose after some use. Moreover, it is shown that the effect of loose-support location on the nonlinear dynamics of the cylinder is significant.

Acknowledgements The authors gratefully acknowledge the support provided by the National Natural Science Foundation of China (No. 10802031). The authors would like to extend their thanks to the anonymous reviewers for their helpful comments.

References

1. Paidoussis, M.P.: Flow-induced vibration in nuclear reactors and heat exchangers: practical experiences and state of knowledge. In: Naudascher, E., Rockwell, D. (eds.) Practical Experiences in Flow-Induced Vibrations, pp. 1–81. Springer, Berlin (1980)
2. Lever, J.H., Weaver, D.S.: A theoretical model for the fluidelastic instability in heat exchanger tube bundles. J. Press. Vessel Technol. **104**, 147–158 (1982)
3. Price, S.J., Paidoussis, M.P.: A single-flexible-cylinder analysis for the fluidelastic instability of an array of flexible cylinders in cross-flow. J. Fluids Eng. **108**, 193–199 (1986)
4. Price, S.J., Paidoussis, M.P.: An improved mathematical model for the instability of cylinder rows subject to cross-flow. J. Sound Vib. **97**, 615–640 (1984)
5. Chen, S.S.: Instability mechanics and stability criteria of a group of circular cylinders subject to cross-flow. J. Vib. Acoust., Stress Reliab. Des. **105**, 51–58 (1983)
6. Lever, J.H., Weaver, D.S.: On the stability of heat exchanger tube bundles, parts I and II. J. Sound Vib. **107**, 375–392, 393–410 (1986)
7. Paidoussis, M.P.: Flow-induced instabilities of cylindrical structures. Appl. Mech. Rev. **40**, 163–175 (1987)
8. Chen, S.S.: A general theory for dynamic instability of tube arrays in cross-flow. J. Fluids Struct. **1**, 35–53 (1987)
9. Price, S.J.: A review of theoretical models for fluidelastic instability of cylinder arrays in cross-flow. J. Fluids Struct. **9**, 463–518 (1995)
10. Price, S.J., Valerio, N.R.: A non-linear investigation of single-degree-of-freedom instability in cylinder arrays subject to cross flow. J. Sound Vib. **137**, 419–432 (1990)
11. Paidoussis, M.P., Li, G.X.: Cross-flow-induced chaotic vibrations of heat-exchanger tubes impacting on loose supports. J. Sound Vib. **152**, 305–326 (1992)
12. de Bedout, J.M., Franchek, M.A., Bajaj, A.K.: Robust control of chaotic vibrations for impacting heat exchanger tubes in crossflow. J. Sound Vib. **227**, 183–204 (1999)
13. Cai, Y., Chen, S.S.: Chaotic vibrations of nonlinearly supported tubes in crossflow. ASME J. Press. Vessel Technol. **115**, 128–134 (1993)
14. Hassan, M., Hayder, M.: Modelling of fluidelastic vibrations of heat exchanger tubes with loose supports. Nucl. Eng. Des. **238**, 2507–2520 (2008)
15. Hassan, M., Weaver, D., Dokainish, M.: A simulation of the turbulence response of heat exchanger tubes in lattice-bar supports. J. Fluids Struct. **16**(8), 1145–1176 (2002)
16. Paidoussis, M.P., Li, G.X., Moon, F.C.: Chaotic oscillations of the autonomous system of a constrained pipe conveying fluid. J. Sound Vib. **135**, 1–19 (1989)
17. Paidoussis, M.P., Li, G.X., Rand, R.H.: Chaotic motions of a constrained pipe conveying fluid: comparison between simulation, analysis and experiment. J. Appl. Mech. **58**, 559–565 (1991)
18. Wang, L.: A further study on the nonlinear dynamics of simply supported pipes conveying pulsating fluid. Int. J. Non-Linear Mech. **44**, 115–121 (2009)